

## **A WIDE-BAND, POLARIZATION-INSENSITIVE AND WIDE-ANGLE TERAHERTZ METAMATERIAL ABSORBER**

**C. Gu, S. Qu, Z. Pei, H. Zhou, and J. Wang**

College of Science  
Air Force Engineering University  
Xi'an 710051, China

**B. Lin**

Institute of Telecommunication and Engineering  
Air Force Engineering University  
Xi'an 710077, China

**Z. Xu**

Electronic Materials Research Laboratory  
Key Laboratory of Ministry of Education  
Xi'an Jiaotong University  
Xi'an 710049, China

**P. Bai and W. Peng**

Synthetic Electronic Information System Research Department  
Air Force Engineering University  
Xi'an 710051, China

**Abstract**—In this paper, a wide-band, polarization-insensitive, wide-angle terahertz metamaterial absorber is presented. Simulated results show that the absorber can achieve polarization-insensitive, wide-angle absorptions in a wide band from 4.15 to 4.85 THz. The retrieved impedance shows that the impedance of the absorber could be tuned, in the absorption band, to match approximatively that of free space on one side and to mismatch on the other side, rendering both the reflectance and transmission minimal and thus the corresponding absorbance maximal. The simulated absorbances under three different

loss conditions suggest that high absorbance is mainly due to the metallic absorption (Ohmic loss). The dielectric loss of the substrate is minor compared with the metallic absorption. The distribution of the surface current density indicates that the electric and magnetic responses are mainly caused by the front structure. This wide-band terahertz metamaterial absorber has potential applications in many functional devices such as microbolometers, thermal detectors, and solar cells.

## 1. INTRODUCTION

Metamaterials (MMs) are artificially designed media composed of subwavelength-engineered units, exhibiting unique electromagnetic properties that are unattainable with natural materials. With MMs, peculiar phenomena such as negative refraction [1, 2] can be obtained. MMs are ideal for the investigation of novel physical phenomena and promising for future applications. Potential applications such as superlensing with a flat slab [3], cloaking [4], miniature antennas [5], and many other novel functional devices have been proposed and studied.

Recently, the design of resonant metamaterial absorbers (MAs) with near-unity absorbance has been proposed at microwave and THz bands [6, 7]. Later, several efforts have been made on MAs to achieve polarization-insensitive absorption [8, 9], wide-angle absorption [10–12] and multiband absorption [13, 14]. These MAs display great absorption capability. However, they are strongly dependent on electromagnetic resonances, thus their bandwidth is rather narrow, no more than 10% relative to the center frequency. This narrowband feature of these MAs limits their potential applications in many functional devices such as microbolometers [15], thermal detectors [16], and solar cells [17, 18]. In this work, a terahertz MA, which is difficult to be achieved by naturally occurring materials, is proposed. The MA is wide-band, polarization-insensitive and wide-angle. Simulated results show that the absorber can achieve polarization-insensitive, wide-angle absorptions in a wide band from 4.15 to 4.85 THz.

## 2. DESIGN AND SIMULATION

A single unit cell of the proposed MA consists of the front structure [Fig. 1(a)], back ring [Fig. 1(b)] and middle substrate. The electric response was caused by the coplanar coupling of metallic structures, while the magnetic response was supplied by the coupling between the front structure and back ring. The magnetic response is similar

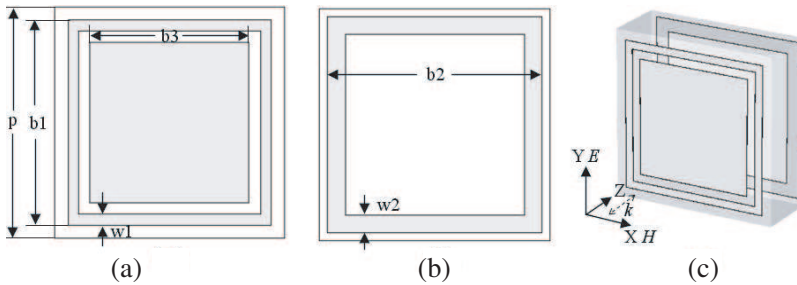


**Figure 1.** The front structure (a), the back ring (b) and the unit cell (c). Geometrical dimensions are:  $b_1 = 9.75 \mu\text{m}$ ,  $w_1 = 0.25 \mu\text{m}$ ,  $b_2 = 12.1 \mu\text{m}$ ,  $w_2 = 1 \mu\text{m}$ ,  $b_3 = 9 \mu\text{m}$  and  $p = 18 \mu\text{m}$ .

to that of short wire pairs [19], resulting from antiparallel currents in parallel metallic segments. The electromagnetic response can be tuned by changing the geometry parameters of the front structure, back ring and spacing between them. To maximize the absorption of the MA, both the transmission and reflection should be minimized. Thus, the impedance of the absorber should be tuned to match approximatively that of free space on one side and mismatch on the other side in the absorption band. This can lead to a minimal reflectance, a minimal transmission and hence a maximal absorbance. Because of the coupling between the back ring and front patch as well as the front ring, there may exist two resonances. The wide-band property of the MA could be realized by making different resonances overlap. The polarization-insensitive and wide-angle property could be realized by improving the symmetry of the unit cell [8]. Because of this, square patches and rings, which have good symmetry, are adopted.

Computer simulation of the MA was performed using the commercial finite difference time domain solver (CST Microwave Studio 2008). The program simulated a single unit cell as shown in Fig. 1(c) with proper boundary conditions, i.e., perfect electric boundary ( $XZ$ -plane) and perfect magnetic boundary ( $YZ$ -plane). The other two boundaries were set to be waveports. By such boundary settings, an infinite MA slab was simulated with plane wave impinging on it. Using CST, the structure of the MA was optimized under normal incidence. The substrate ( $\epsilon_r = 4.9$ , loss tangent  $\tan \delta = 0.025$ ) is  $5 \mu\text{m}$  thick. By the simulation, the frequency-dependent  $S$  parameters,  $S_{11}$ ,  $S_{21}$ ,  $S_{22}$  and  $S_{12}$ , can be obtained. The frequency-dependent absorbances under three different front structures were calculated by  $A(\omega) = 1 - |S_{11}|^2 - |S_{21}|^2$ , as shown in Fig. 2.

From Fig. 2, when the front structure is composed of both the patch and the ring, there is a wide band from 4.15 to 4.85 THz with

strong absorption. The absorption bandwidth, in which the absorbance is greater than 90%, is 0.70 THz. There are two resonances located at 4.28 and 4.68 THz, respectively. When the front structure is only the patch, there is a 64.4% absorption peak at 4.51 THz, which is due to the resonance resulting from the coupling between the back ring and the front patch. The absorption bandwidth, in which the absorbance is greater than 50%, is 0.46 THz. When the front structure is only the ring, there is a 87.3% absorption peak at 4.10 THz, which is due to the resonance resulting from the coupling between the back ring and the front ring. The absorption bandwidth, in which the absorbance is greater than 50%, is 0.49 THz. These results indicate that the wide-band property could be realized by making different resonances overlap. Meanwhile, when the front structure includes both the patch and the ring, the low-frequency resonance at 4.28 THz arises mainly from the coupling between the back ring and the front ring, and the high-frequency resonance at 4.68 THz is mainly resulted from the coupling between the back ring and the front patch.

Real parts of the complex wave impedance ( $Z$ ) can be retrieved from the simulated  $S$  parameters for two different transmission directions [20], as shown in Fig. 3. When the wave propagates along  $+Z$ , the average value of real parts of the impedance in 4.15–4.85 THz is 0.8, and it matches approximately the impedance of free space on the front side. When the wave propagates along  $-Z$ , the average value of real parts of the impedance in 4.15–4.85 THz is 0.04, which does not match the impedance of free space. These results suggest that

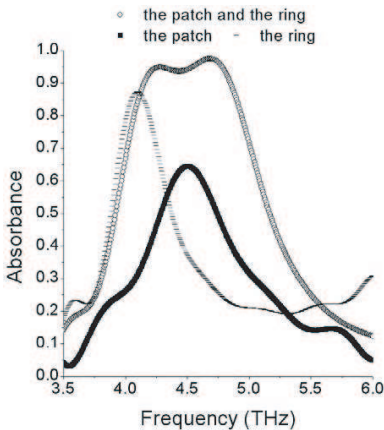


**Figure 2.** Simulated absorbances of the MA for three different front structures.

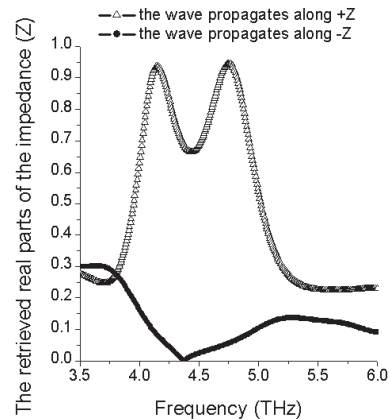


**Figure 3.** Retrieved real parts of the wave impedance.

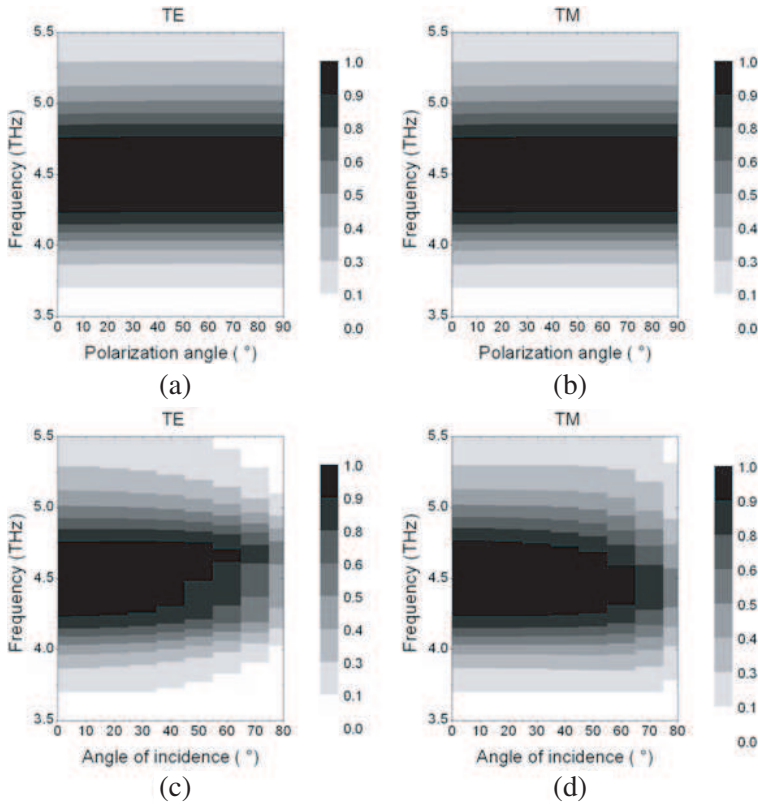


**Figure 4.** Simulated absorbance values under different polarization angles for TE (a) and TM (b) waves. Simulated absorbance values under different angles of incidence for TE (c) and TM (d) waves.

the impedance of the absorber could be tuned to match approximately that of free space on one side while to mismatch on the other side in the absorption band. This can lead to minimal reflectance and transmission, and thus to maximal absorbance.

Moreover, the configuration in Fig. 1 is polarization-insensitive and wide-angle. Evidence of this can be obtained from Fig. 4, which shows the simulated absorbances under different polarization angles and different angles of incidence for TE and TM waves. Figs. 4(a) and (b) show that the absorbances under different polarization angles for TE and TM waves are almost the same. Figs. 4(c) and (d) show that the absorbance values are not significantly influenced by the angle of incidence for TE and TM plane waves. For the TE wave, the absorbances in the absorption band are almost unchanged under

the  $55^\circ$  angle of incidence. For the TM wave, the absorbances in the absorption band are nearly unchanged under the  $65^\circ$  angle of incidence. These results suggest that the MA is polarization-insensitive and wide-angle because of the excellent symmetry of the unit cell [8].

### 3. THE POWER LOSS AND SURFACE CURRENT

It is also interesting to explore the power loss in the MA since it can provide information about how and where the absorption happens. Fig. 5 compares the absorbances under three different loss conditions. When the substrate is lossy and the metal is copper, the 90% absorption bandwidth is 0.70 THz and an averaged 91.4% energy is absorbed. When the substrate is loss-free and the metal is copper, the 90% absorption bandwidth is still 0.70 THz, and an averaged 91.4% energy is consumed, too. When the substrate is lossy and the metal is perfect electric conductor (PEC), only an averaged 72.6% energy is consumed in the 60% absorption band. The simulated absorbances under three different loss conditions suggest that high absorbance is mainly due to the metallic absorption (Ohmic loss). The dielectric loss of the substrate is minor compared with the metallic absorption. This is different from previous studies on frequency selective surfaces (FSSs) where metallic absorption was relatively insignificant in comparison with dielectric loss of the substrate [21].

The distribution of the surface current in the MA was also calculated. In Fig. 6, a vector plot of the surface current density in the MA at 4.5 THz is presented. From Fig. 6(a), there are obvious anti-parallel currents between the patch and the ring in the front structure.

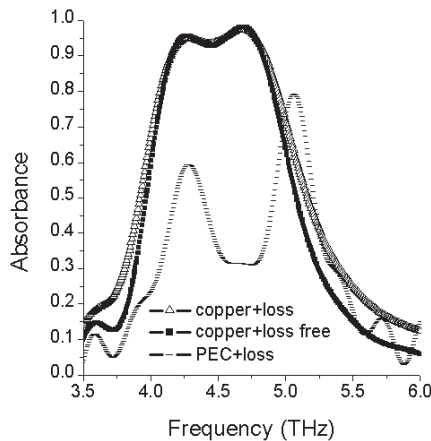


**Figure 5.** Simulated absorbances under three different loss conditions.

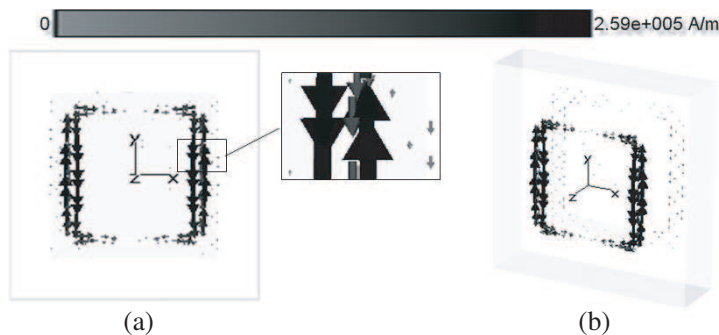


**Figure 6.** The distribution of the surface current density in the MA at 4.5 THz. (a) The front view; (b) the 3-D view.

From Fig. 6(b), comparatively small anti-parallel currents between the front structure and the back ring can be seen. It can be concluded that the magnetic response is supplied by the front structure which is also the chief supplier of electric response.

#### 4. CONCLUSION

In this work, a wide-band, polarization-insensitive, wide-angle terahertz metamaterial absorber is presented. The retrieved impedance shows that the impedance of the absorber could be tuned in the absorption band, to match approximatively that of free space on one side and to mismatch on the other side, rendering both the reflectance and transmission minimal and thus the corresponding absorbance maximal. The simulated absorbances under different polarization angles validate the polarization-insensitive property of the MA. The simulated absorbances under different angles of incidence validate the wide-angle property of the MA. The absorption mechanism was investigated by simulating absorbance values under three different loss conditions, which shows that high absorbance is mainly due to the metallic absorption (Ohmic loss). The dielectric loss of the substrate is minor compared with the metallic absorption. The distribution of the surface current density indicates that the magnetic response is supplied by the front structure which is also the chief supplier of electric response. Such a wide-band THz MA may find numerous applications ranging from the active element in a thermal detector to THz stealth technology.

## ACKNOWLEDGMENT

This project is supported by the National Natural Science Foundation of China under Grants 50632030, 60871027, 60901029 and 61071058 and in part by the 973 Project of Science and Technology Ministry of China under Grant 2009CB613306.

## REFERENCES

1. Veselago, V. G., "The electrodynamics of substances with simultaneously negative values of  $\varepsilon$  and  $\mu$ ," *Sov. Phys. Usp.*, Vol. 10, 509, 1968.
2. Shelby, R. A., D. R. Smith, and S. Schultz, "Experimental verification of a negative index of refraction," *Science*, Vol. 292, No. 5514, 77–79, 2001.
3. Smith, D. R., D. Schurig, M. Rosenbluth, S. Schultz, S. A. Ramakrishna, and J. B. Pendry, "Limitations on subdiffraction imaging with a negative refractive index slab," *Appl. Phys. Lett.*, Vol. 82, No. 10, 1506–1508, 2003.
4. Schurig, D., J. J. Mock, B. J. Justice, S. A. Cummer, J. B. Pendry, A. F. Starr, and D. R. Smith, "Metamaterial electromagnetic cloak at microwave frequencies," *Science*, Vol. 314, No. 5801, 977–980, 2006.
5. Enoch, S., G. Tayeb, P. Sabouroux, N. Guérin, and P. Vincent, "A metamaterial for directive emission," *Phys. Rev. Lett.*, Vol. 89, No. 21, 213902, 2002.
6. Landy, N. I., S. Sajuyigbe, J. J. Mock, D. R. Smith, and W. J. Padilla, "Perfect metamaterial absorber," *Phys. Rev. Lett.*, Vol. 100, 207402, 2008.
7. Tao, H., N. I. Landy, C. M. Bingham, X. Zhan, R. D. Averitt, and W. J. Padilla, "A metamaterial absorber for the terahertz regime: Design, fabrication and characterization," *Opt. Express*, Vol. 16, No. 10, 7181–7188, 2008.
8. Landy, N. I., C. M. Bingham, T. Tyler, N. Jokerst, D. R. Smith, and W. J. Padilla, "Design, theory, and measurement of a polarization insensitive absorber for terahertz imaging," *Phys. Rev. B*, Vol. 79, No. 12, 125104, 2009.
9. Zhu, B., Z. Wang, C. Huang, Y. Feng, J. Zhao, and T. Jiang, "Polarization insensitive metamaterial absorber with wide incident angle," *Progress In Electromagnetics Research*, Vol. 101, 231–239, 2010.
10. Tao, H., C. M. Bingham, A. C. Strikwerda, D. Pilon,



- D. Shrekenhamer, N. I. Landy, K. Fan, X. Zhang, W. J. Padilla, and R. D. Averitt, "Highly flexible wide angle of incidence terahertz metamaterial absorber: Design, fabrication, and characterization," *Phys. Rev. B*, Vol. 78, 241103 R, 2008.
11. Avitzour, Y., Y. A. Urzhumov, and G. Shvets, "Wide-angle infrared absorber based on a negative-index plasmonic metamaterial," *Phys. Rev. B*, Vol. 79, No. 4, 045131, 2009.
  12. Lagarkov, A. N., V. N. Kisel, and V. N. Semenenko, "Wide-angle absorption by the use of a metamaterial plate," *Progress In Electromagnetics Research Letters*, Vol. 1, 35–44, 2008.
  13. Wen, Q. Y., H. W. Zhang, Y. S. Xie, Q. H. Yang, and Y. L. Liu, "Dual band terahertz metamaterial absorber: Design, fabrication, and characterization," *Appl. Phys. Lett.*, Vol. 95, No. 24, 241111, 2009.
  14. Tao, H., C. M. Bingham, D. Pilon, K. Fan, A. C. Strikwerda, D. Shrekenhamer, W. J. Padilla, X. Zhang, and R. D. Averitt, "A dual band terahertz metamaterial absorber," *J. Phys. D: Appl. Phys.*, Vol. 43, 225102, 2010.
  15. Mauskopf, P. D., J. J. Bock, H. Del Castillo, W. L. Holzapfel, and A. E. Lange, "Composite infrared bolometers with Si<sub>3</sub>N<sub>4</sub> micromesh absorbers," *Appl. Opt.*, Vol. 36, No. 4, 765–771, 1997.
  16. Parsons, A. D. and D. J. Pedder, "Thin-film infrared absorber structures for advanced thermal detectors," *J. Vac. Sci. Technol. A*, Vol. 6, No. 3, 1686–1689, 1988.
  17. Rand, B. P., P. Peumans, and S. R. Forrest, "Long-range absorption enhancement in organic tandem thin-film solar cells containing silver nanoclusters," *J. Appl. Phys.*, Vol. 96, No. 12, 7519–7526, 2004.
  18. Pillai, S., K. R. Catchpole, T. Trupke, and M. A. Green, "Surface plasmon enhanced silicon solar cells," *J. Appl. Phys.*, Vol. 101, No. 9, 093105, 2007.
  19. Zhou, J. F., L. Zhang, G. Tuttle, T. Koschny, and C. M. Soukoulis, "Negative index materials using simple short wire pairs," *Phys. Rev. B*, Vol. 73, No. 4, 041101, 2006.
  20. Chen, X. D., T. M. Grzegorzcyk, B. I. Wu, J. P. Jr, and J. A. Kong, "Robust method to retrieve the constitutive effective parameters of metamaterials," *Phys. Rev. E*, Vol. 70, No. 1, 016608, 2004.
  21. Reynolds, J. E, B. A. Munk, J. B. Pryor, and R. J. Marhefka, "Ohmic loss in frequency selective surface," *J. Appl. Phys.*, Vol. 93, No. 9, 5346–5358, 2003.